

## Theoretical calculations of phase transitions and optical properties of solid iodine under high pressures

This article has been downloaded from IOPscience. Please scroll down to see the full text article.

2008 J. Phys.: Condens. Matter 20 175225

(<http://iopscience.iop.org/0953-8984/20/17/175225>)

View [the table of contents for this issue](#), or go to the [journal homepage](#) for more

Download details:

IP Address: 129.252.86.83

The article was downloaded on 29/05/2010 at 11:38

Please note that [terms and conditions apply](#).

# Theoretical calculations of phase transitions and optical properties of solid iodine under high pressures

Xiaojiao San, Liancheng Wang, Yanming Ma, Zhiming Liu,  
Tian Cui<sup>1</sup>, Bingbing Liu and Guangtian Zou

National Laboratory of Superhard Materials, Jilin University, Changchun 130012,  
People's Republic of China

E-mail: [cuitian@jlu.edu.cn](mailto:cuitian@jlu.edu.cn)

Received 18 January 2008, in final form 17 March 2008

Published 7 April 2008

Online at [stacks.iop.org/JPhysCM/20/175225](http://stacks.iop.org/JPhysCM/20/175225)

## Abstract

The structural stability and optical properties of solid iodine under pressure have been studied using the *ab initio* pseudopotential plane-wave method. The dependence of lattice parameters on pressure indicates that the first structural phase transition from phase I to phase V occurs at about 20 GPa. From the pressure dependence of our elastic constants for solid iodine in phase I, it is found that the first structural transformation from molecular phase I to the intermediate phase V occurs at about 20 GPa due to the softening of the elastic constant  $C_{44}$ , which is very close to the transition pressure of 20 GPa obtained by geometry optimizations and 23.2 GPa obtained by experimental measurements. The optimized structure for phase V is a face-centered orthorhombic (fco) phase with equal interatomic distances  $d_1 = d_2 = d_3$ , but this fco structure is mechanically unstable, with shear elastic stiffness coefficient  $C_{44} < 0$ . To understand the modulated phase V, we use a periodic crystal structure to mimic the incommensurate phase V and obtain some quantitative information. In our calculation, the modulated phase is thermodynamically and mechanically stable. It is believed that phase V is not a monatomic phase but an intermediate state between a molecular and a monatomic state.

(Some figures in this article are in colour only in the electronic version)

## 1. Introduction

Dense diatomic molecular solids such as oxygen [1–3], nitrogen [4], and iodine [5–9] have been investigated intensively for decades. The successive pressure-induced transitions in these diatomic molecular solids, i.e. metallization, molecular dissociation, and superconductivity, make the research field more attractive and challenging. Moreover, such investigations can give important and valuable information for understanding the dense metallic hydrogen.

The structure of solid iodine has been studied experimentally using x-ray diffraction or Raman scattering techniques. It is known that the molecular phase (phase I) and the monatomic phase (phase II) belong to the space group  $Cmca$  and  $Immm$ , respectively. The latest experimental observation by the Raman

scattering technique [10] showed that the monatomic phase II occurs above 30 GPa for iodine, which is higher than that reported in the early experimental and theoretical investigations [5–9]. In recent experimental studies by using the x-ray diffraction technique [11], an intermediate phase V between the molecular phase I and the monatomic phase II is observed for iodine at 23.2 GPa. Moreover, the results from both the x-ray diffraction and Raman scattering demonstrate that coexistence of phase I and V is in a pressure range from 23 to 24 GPa, and phase V of iodine is shown to be incommensurate. In this incommensurate phase iodine atoms form a two-dimensional network in the  $a$ – $b$  plane. The modulation wave is transverse, which periodically shifts the atoms in the direction parallel to the  $b$ -axis. The wavelength  $1/k$  of the modulation wave is not a multiple of the length of the  $a$ -axis, making the structure incommensurate. In terms of the super space-group representation, this structure is written as  $Fmm2(\alpha 00)0s0$ , which

<sup>1</sup> Author to whom any correspondence should be addressed.

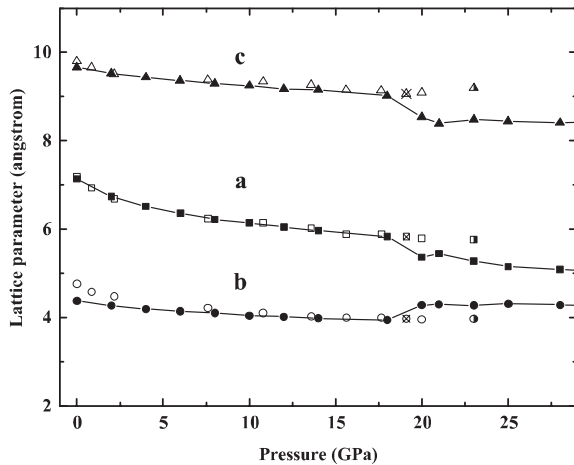


**Figure 1.** Pressure dependence of the lattice parameters obtained by an x-ray experiment from [27, 28, 11] (open symbols, partly shadow symbols, and crossed symbols, respectively) and the present calculations (solid symbols).

is equivalent to  $F2mm(00\gamma)0s0$  in the literature [12]. Their measurements show that no diatomic molecules exist in phase V, however, it is difficult to decide whether phase V has molecular or monatomic character.

As for the molecular phase of iodine, the previous experiments of Drickamer [13, 14] in 1965 and 1966 revealed the metallic behavior of molecular iodine under pressures, and observed that the metallization of iodine in the direction perpendicular to the iodine molecule plane occurred earlier than in the direction parallel to the iodine molecule plane. The metal–insulator (MI) transition has been found at 16 GPa. The gap closure in molecular phase I of solid iodine is observed before the molecular dissociation. Subsequently, several theoretical works using empirical models [15–17] and first-principles calculations [18–22] have been reported.

Up to now, there has been no comprehensive theoretical research on phase V and phase II of solid iodine. The aim of this work is to have more insight into the nature of the phase transitions. The metallization, the molecular dissociation, and the phase transition from phase I to phase V are studied by using the *ab initio* pseudopotential plane-wave (PW) method [23]. It is believed that the structural phase transition from molecular phase I to intermediate phase V is induced by the softening of elastic constant  $C_{44}$ . In our calculations, even though incommensurate phase V is simulated by a periodic crystal structure, the modulated phase is more thermodynamically and mechanically stable and some important information has been obtained. The results of the optical properties indicate that phase V is not a monatomic phase but an intermediate state between a molecular and a monatomic state. These theoretical results should enhance our microscopic understanding of the solid.

## 2. Computational details

The geometries of the structure including cell parameters as well as atomic positions for solid iodine starting from an eight-atom unit cell are optimized under different pressures in the

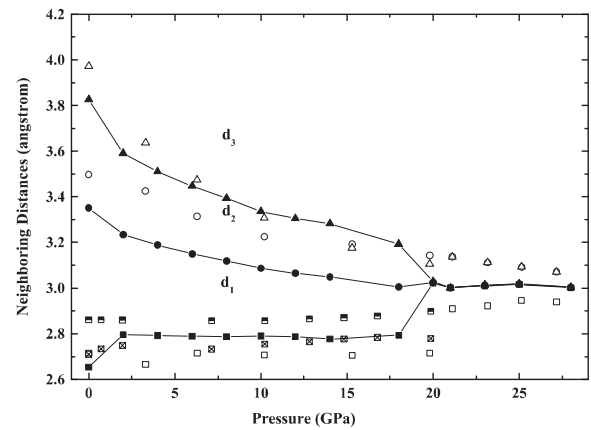


**Figure 2.** The changes of the first, the second, and the third neighbor interatomic distances inside the iodine molecule plane versus pressure. Our calculated results are represented by the solid symbols, the full-potential LMTO from [21] results are represented by the partly shadow symbols, the experimental measurements from [7, 27] are represented by the open symbols and the crossed symbols, respectively.

range of 0–32 GPa by performing the *ab initio* pseudopotential PW method with norm-conserving pseudopotentials [24]. The cutoff radius of the pseudopotentials is 2.30 bohr. A convergence test gives an energy cutoff of 440 eV and  $0.03 \text{ \AA}^{-1}$  Monkhorst–Pack grid spacing is used in the electronic Brillouin zone (BZ) integration. Exchange and correlation effects are treated within the local-density approximation (LDA) [25] available in CASTEP code [26]. Calculations of the elastic constants require a very high degree of precision because the energy differences involved are of the order of about 1 mRyd.

## 3. Results and discussion

### 3.1. Structural stability

The calculated lattice parameter as a function of pressure is plotted in figure 1, together with the experimental measurements [11, 27, 28]. It is found that in the range of 0–18 GPa our calculated lattice parameters  $a$ ,  $b$ ,  $c$  are very close to those obtained by an x-ray experiment, and our calculated bulk modulus of molecular iodine at ambient pressure is 14.24 GPa, which is much closer to the experimental value of 13.73 GPa [29, 30] than the other theoretical value of 13.13 GPa [22]. The inflexion provides a signal that the structural phase transition from phase I to phase V may occur at 20 GPa. We present the calculated LDA interatomic distances of iodine in the iodine molecule plane and compare them with the other theoretical results [21] and experimental measurements [7, 27] in figure 2. In the range of 0–18 GPa, the second and the third neighboring distances decrease significantly with increasing pressure, while the nearest-neighboring distance, i.e. the bond length, changes only slightly. In solid bromine, the significant changes of molecular bond length with pressure in phase I have been found by x-ray measurements [31] recently, but in our calculations,

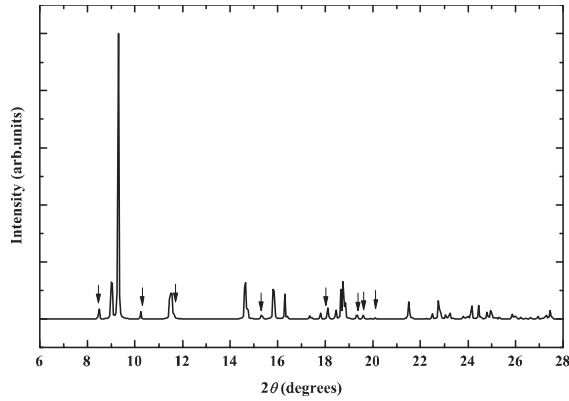


**Figure 3.** Powder x-ray diffraction pattern of our calculated structure of solid iodine at 21 GPa. The arrows indicate the experimental satellite reflection peaks of the incommensurate phase of iodine at 24.6 GPa from [11].

we do not observe a similar phenomenon in solid iodine. At 20 GPa, the bond length and the second neighboring distance in the fco phase get larger abruptly and the relaxed geometry shows that the differences of the three kinds of interatomic distances vanish, namely  $d_1 = d_2 = d_3$ .

In order to make a comparison among different phases, we exchange the  $c$ - and  $a$ -axis in phase V and II, and keep the iodine molecule plane in the  $c$ - $b$  plane. Since phase V of iodine is observed to be incommensurate by the x-ray diffraction technique [11], we mimic it by a modulation wavevector  $k_z = 1/4$  or  $1/6$  with the fco lattice obtained by geometry optimization from the  $Cmca$  directly, which is based on the investigation in [11]. The modulation wavevector is along the  $c$ -axis with displacements along the  $b$ -axis which is perpendicular to the wavevector. The maximum displacement of modulations in the  $c$ - $b$  plane is  $B(y) = 0.0532$  [11]. The modulated structure is fully optimized and the displacement of modulation decreases with increasing pressure. The atomic separations in this optimal structure are in the range 2.86–3.11 Å, which are compared with the experimental measurements. Figure 3 shows the x-ray diffraction pattern of our modulated structure of iodine at 21 GPa. The satellite reflection peaks of the experimental measurements at 24.6 GPa from [11] is labeled by arrows. The strong peaks and a number of weak peaks are consistent with the experimental data. Therefore, the incommensurate phase V mimicked by this periodic crystal structure is feasible. As for the monatomic phase II with the body-centered orthorhombic (bco) lattice, we adopt the structural information mentioned in the x-ray diffraction measurements [11]. All these structures mentioned above are plotted in figures 4(a)–(d).

The enthalpy differences for the above-mentioned structures ( $Cmca$ , fco, modulated, and bco) are shown in figure 5. The fco phase has lower enthalpy than the  $Cmca$  phase after 20 GPa, indicating the occurrence of the phase transition, which is consistent with the results of our geometry optimization. As for the modulated phase, it has lower enthalpy than the fco phase from 19 to 29 GPa, suggesting that the modulated phase is more thermodynamically stable in this pressure range. Above 29 GPa, the bco phase has the

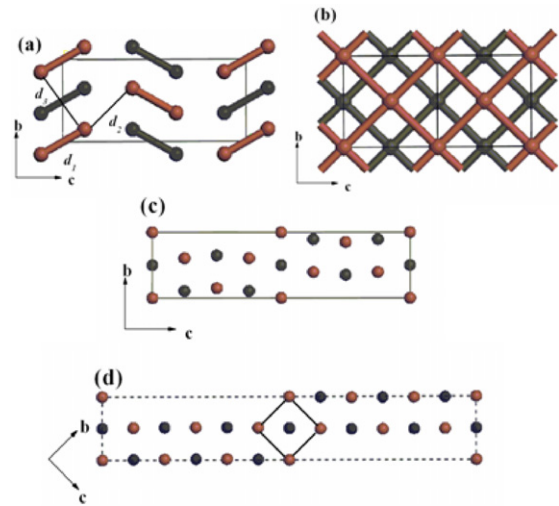


**Figure 4.** The structures of iodine in molecular phase I, the fco obtained from geometry optimization, the modulated fco which has a modulation wavevector  $k_z = 1/4$ , and the monatomic phase II are plotted in (a)–(d), respectively. The atoms shown by colored spheres are on the same plane and those by black spheres are on an adjacent plane above or below the plane with separation  $a/2$  (Colour online).

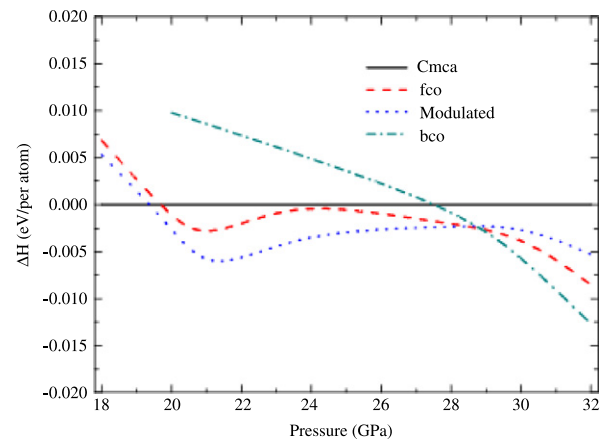


**Figure 5.** Calculated enthalpy differences of the four phases of solid iodine considered in this work relative to that of the  $Cmca$  phase as a function of pressure.

lowest enthalpy, which is close to the experimental result of 30 GPa [11].

As we know, the elastic constants of materials depict the response to an applied stress, which provides valuable information about the binding characteristic between adjacent atomic planes, the anisotropic character of binding, and structural stability. Hence, for understanding the mechanical stability of a stressed lattice and the phase transition of solid iodine from phase I to phase V, we have calculated the elastic constants of solid iodine in phase I at ambient and high hydrostatic pressure by using the CASTEP package [26].

The stress tensor relates to the strain tensor by Hooke's law with the elastic stiffness coefficients as proportional coefficients. Since the stress and strain tensors are symmetric, the most general elastic stiffness tensor has only 21 non-zero independent components. For an orthorhombic

**Table 1.** The calculated elastic stiffness constants  $C_{ij}$  of solid iodine in phase I (*Cmca*), fco, and the modulated phase at LDA levels at zero temperature.

	$P$ (GPa)	$C_{11}$	$C_{22}$	$C_{33}$	$C_{44}$	$C_{55}$	$C_{66}$	$C_{12}$	$C_{13}$	$C_{23}$
<i>Cmca</i>	0	20.55	30.75	65.78	38.83	3.83	8.77	5.67	-1.62	29.56
	8	92.31	86.32	152.94	91.30	16.76	36.83	31.76	7.18	82.86
	16	120.51	188.89	173.87	71.87	64.42	46.88	55.73	55.29	126.30
	20	122.81	205.40	193.55	-2.61	76.68	77.33	64.70	90.31	135.05
fco	20	67.73	156.70	167.200	-107.67	48.41	44.16	112.00	102.29	140.52
Modulated	20	142.84	191.13	169.25	44.67	73.48	70.85	51.42	93.35	164.67

crystal, they are reduced to nine components, i.e.  $C_{11}$ ,  $C_{22}$ ,  $C_{33}$ ,  $C_{44}$ ,  $C_{55}$ ,  $C_{66}$ ,  $C_{12}$ ,  $C_{13}$ , and  $C_{23}$ . The pressure dependence of the calculated elastic constants of solid iodine in phase I at the LDA level [25], and the elastic constants in fco and modulated phase at 20 GPa are summarized in table 1.

The elastic constant  $C_{11}$  ( $C_{22}$  and  $C_{33}$ ) represents the elasticity in length. The elastic constants  $C_{12}$  ( $C_{13}$  and  $C_{23}$ ) and  $C_{44}$  ( $C_{55}$  and  $C_{66}$ ) are related to the elasticity in shape, which are shear constants. A transverse strain causes a change in shape without a change in volume. From table 1, it is interesting to note that the value of  $C_{44}$  is increasing with pressure under the lower pressure range, and then decreases with increasing pressure. The values of shear moduli  $C_{44}$  at 20 GPa become negative, indicating that the structure of phase I is unstable by the Born stability criteria [32].

From our elastic constants of solid iodine in phase I under pressures, the phase I–phase V structural transformation happens at about 20 GPa, which is consistent with the pressure of 20 GPa obtained by our geometry optimizations and equation of states results. It is also shown that softening of the elastic constant  $C_{44}$  drives the phase transition from molecular phase I to the intermediate phase V.

The elastic constants of the fco and modulated phases at 20 GPa are also listed in table 1. The value of  $C_{44}$  of the fco phase is negative, suggesting that the fco structure is mechanically unstable, while the modulated phase in our calculation is mechanically and thermodynamically stable.

### 3.2. Metallization

The fundamental band gap of iodine versus pressure is plotted in figure 6. For convenience, a scaled pressure  $P/P_c$  is used, where  $P_c$  equals 16 GPa. As we know, under lower pressures, the LDA gap is underestimated very obviously. But with pressure increase, this underestimation decreases gradually. At 0 GPa, our LDA gap of solid iodine is about 1.15 eV, while the experimental value is about 1.3 eV [33]. It shows that our PW calculated band gap is much closer to the experimental measurements than the other theoretical results of Miao *et al* [22], due to the smaller cutoff radii of the pseudopotential used in our calculations. The band structures of solid iodine at 0 and 16 GPa are shown in figures 7(a) and (b), respectively. The band gap closes in some special symmetry points at 16 GPa, showing the metallization of iodine, in agreement with the early experimental and theoretical results [17, 33].

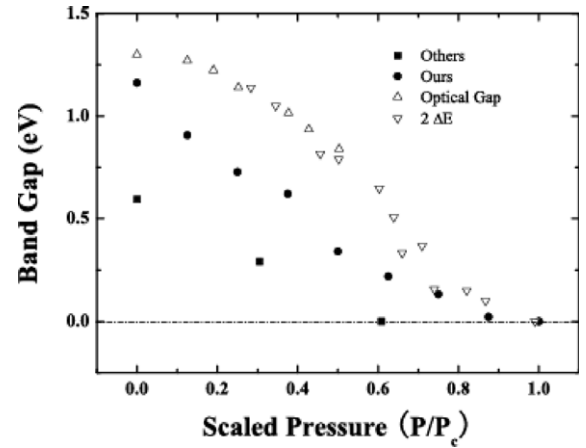


**Figure 6.** The fundamental band gap of iodine versus pressure. Other calculated results [22] and the present calculations are represented by the solid squares and the solid circles, respectively. The experimental measurements obtained from the corrected optical gap and the activation energy for electrical conductivity [33] are represented by the up-triangles and the down-triangles, respectively. For convenience, a scaled pressure  $P/P_c$  is used with  $P_c$  equal to 16 GPa.

### 3.3. The analysis of the molecular dissociation

For understanding the molecular dissociation process of solid iodine induced by pressure, we investigate the electron densities of solid iodine at different pressures. It is indicated that bonding electrons between two iodine atoms can be found in phase I, indicating molecular character in this phase. With increasing pressure, some electrons move from the intramolecular region to the intermolecular region. The electron population gradually becomes similar around every atom in the same plane with increasing pressure. When pressure is larger than 20 GPa, the inter and intramolecular bonds in the modulated phase cannot be distinguished clearly, but only from the population of electron density; we still cannot conclude quantitatively whether a monatomic phase forms or not when the molecular dissociation starts.

### 3.4. Optical properties

The calculated  $\epsilon_2(\omega)$ , which is an imaginary part of the dielectric function of solid iodine as a function of the photon energy, is shown in figures 8(a)–(d), where the solid and dash-dotted lines represent the data of incident radiation with the linear polarization along the [010] and [001] directions (parallel to the iodine molecule plane), respectively,

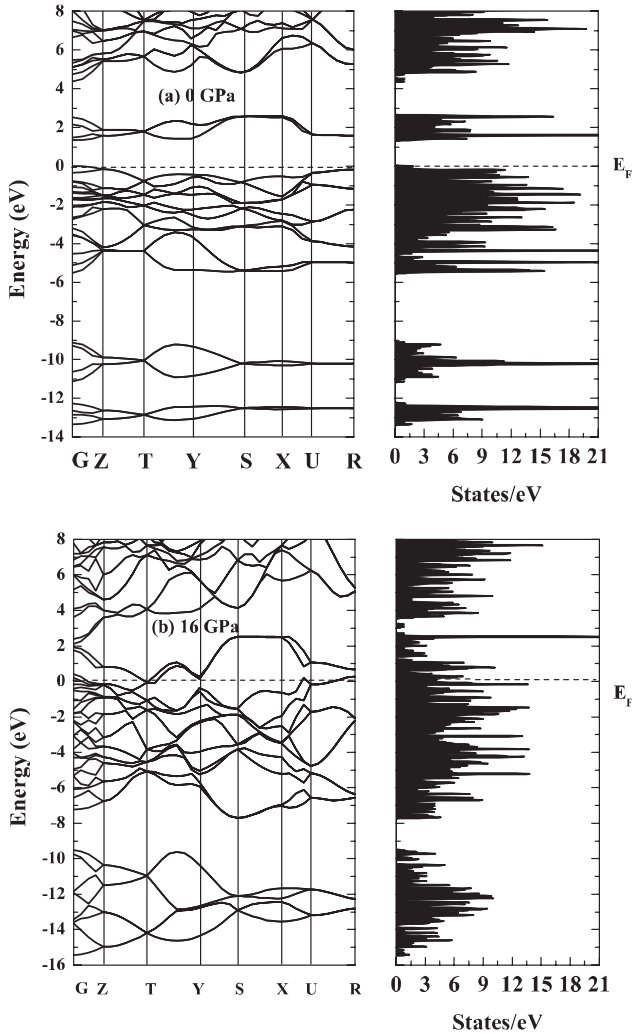


**Figure 7.** Calculated energy band structure of iodine along the high-symmetry directions in the BZ, under 0 and 16 GPa, respectively.

and the dashed lines represent the results with the [100] polarization (perpendicular to the iodine molecule plane). In our calculations, we do not consider the intraband contribution to the optical properties, which affects mainly the low energy infrared part of the spectra.

The results of phase I are plotted in figure 8(a). At 0 GPa, in the [100] polarization, the  $\epsilon_2(\omega)$  has only one main peak at about 7.5 eV and with a shoulder above it, while in the [010] and [001] polarizations, it has two main peaks at about 2.5 and 7.5 eV respectively, implying that there is one inherent frequency in the [100] polarization, while two in the [010] and [001] polarization. With increasing pressure, the intensity of the peak at about 2.5 eV increases gradually. In the case of the modulated phase V shown in figures 8(b) and (c), there are two inherent frequencies in all the three polarizations. The intensity of the first peak of  $\epsilon_2(\omega)$  at about 2.5 eV in all the three polarizations increases largely at 21 GPa, especially in the [001] polarization, and the order of the intensity of the peaks in the three polarizations is consistent with that in the molecular phase I. However, the first peak of  $\epsilon_2(\omega)$  at about 2.5 eV in

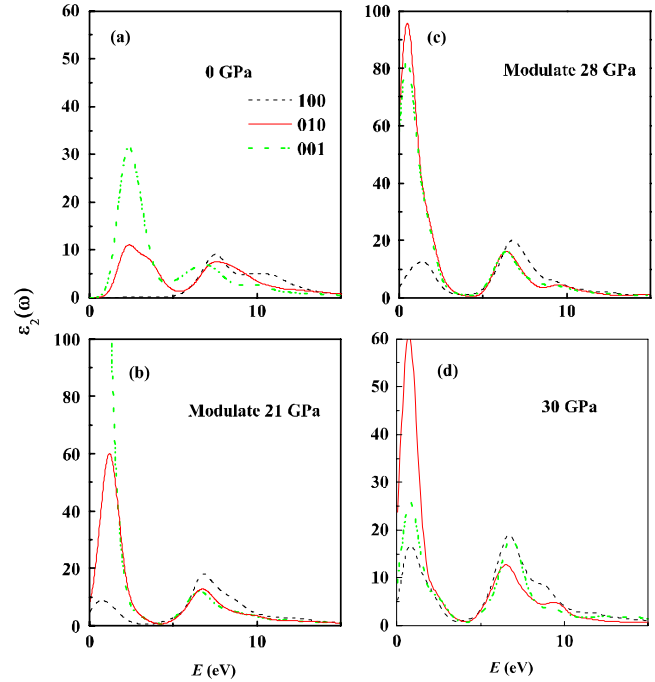


**Figure 8.** Calculated imaginary part of the dielectric function of iodine as a function of the photon energy under 0, 21, 28, and 30 GPa, respectively.

the [010] polarizations largely increases and that in the [001] polarization decreases with further increase of pressure, which makes the first main peak of  $\epsilon_2(\omega)$  located below 2.5 eV in the [010] polarization become stronger than that in the [001] polarization at 28 GPa. The calculated  $\epsilon_2(\omega)$  for phase II is shown in figure 8(d). It is clear that there are two inherent frequencies in all the three polarizations. Furthermore, the first main peak of  $\epsilon_2(\omega)$  in the [010] polarization is the strongest one in the three polarizations, which is consistent with the case of the modulated phase V at 28 GPa.

From figure 8, we can see that the modulated phase V has more molecular characters under lower pressures, but it has more monatomic characters under higher pressures. It is believed that phase V is not a monatomic phase but an intermediate state between a molecular and a monatomic state. These optical results can be used to distinguish phase V and monatomic phase II.

#### 4. Conclusions

In this work, we have investigated atomic structure, the electronic and optical properties of solid iodine under pressures from 0 to 32 GPa using the *ab initio* pseudopotential plane-wave method. The pressure dependence of the lattice parameters indicates that the structural phase transition from phase I to phase V occurs at 20 GPa. It is also shown that softening of the elastic constant  $C_{44}$  is associated with this phase transition. We use a simple periodic structure to simulate incommensurate phase V, which is thermodynamically and mechanically stable in the pressure range from about 19 to 29 GPa. From the calculated electronic and optical properties,

it is found that the modulated phase V is not a monatomic state, which has more molecular characteristics under lower pressures but more monatomic characteristics under higher pressures.

## Acknowledgments

This work was supported by the National Natural Science Foundation of China under Grant Nos 10574053 and 10674053, 2004 NCET and 2003 EYTP of MOE of China, the National Basic Research Program of China, Grant Nos 2005CB724400 and 2001CB711201, the Cultivation Fund of the Key Scientific and Technical Innovation Project (Grant No. 2004-295) and the 2007 Cheung Kong Scholars Programme of China.

## References

- [1] Desgreniers S, Vohra Y K and Ruoff A L 1990 *J. Phys. Chem.* **94** 1117
- [2] Shimizu K, Suhara K, Ikumo M, Eremets M and Amaya K 1998 *Nature* **393** 767
- [3] Goncharov A F, Gregoryanz E, Mao H K, Liu Z and Hemley R J 2000 *Phys. Rev. Lett.* **85** 1262
- [4] Eremets M, Hemley R J, Mao H K and Gregoryanz E 2001 *Nature* **411** 170
- [5] Shimomura O, Takemura K, Fujii Y, Minomura S, Mori M, Noda Y and Yamada Y 1978 *Phys. Rev. B* **18** 715
- [6] Takemura K, Minomura S, Shimomura O and Fujii Y 1980 *Phys. Rev. Lett.* **45** 1881
- [7] Takemura K, Minomura S, Shimomura O, Fujii Y and Axe J D 1982 *Phys. Rev. B* **26** 998
- [8] Shimomura O, Takemura K and Aoki K 1982 *High Pressure in Research and Industry* ed C M Backman *et al* (Uppsala: Arkitektkopia) p 272
- [9] Hayashi Y, Fujii Y, Fujihisa H, Aoki K, Yamawaki H, Shimomura O and Takemura K 1982 *Recent Trends in High Pressure Research* ed A K Singh (New Delhi: Oxford IBH) p 119
- [10] Kume T, Hiraoka T, Ohya Y, Sasaki S and Shimizu H 2005 *Phys. Rev. Lett.* **94** 065506
- [11] Takemura K, Sato K, Fujihisa H and Onoda M 2003 *Nature* **423** 971
- [12] Wilson A J C and Prince E 1999 *International Tables for Crystallography* 2nd edn vol C (Dordrecht: Kluwer Academic) pp 914–26
- [13] Drickamer H G 1965 *Solid State Physics* vol 17, ed F Seitz *et al* (New York: Academic) p 1
- [14] Drickamer H G, Lynch R W, Clendenen R L and Perez-Albuerne E A 1966 *Solid State Physics* vol 19, ed F Seitz *et al* (New York: Academic) p 135
- [15] Siringo F, Pucci R and March N H 1988 *Phys. Rev. B* **37** 2491
- [16] Pucci R, Siringo F and March N H 1988 *Phys. Rev. B* **38** 9517
- [17] Siringo F, Pucci R and March N H 1988 *Phys. Rev. B* **38** 9567
- [18] Sakamoto H, Shirai M and Suzuki N 1995 *J. Phys. Soc. Japan* **64** 3860
- [19] Orita N, Niizeki K, Shindo K and Tanaka H 1992 *J. Phys. Soc. Japan* **61** 4502
- [20] Yamaguchi K and Miyagi H 1998 *Phys. Rev. B* **57** 11141
- [21] Miyagi H, Yamaguchi K, Matsuo H and Mukose K 1998 *J. Phys.: Condens. Matter* **10** 11203
- [22] Miao M S, van Doren V E and Martins J L 2003 *Phys. Rev. B* **68** 094106
- [23] Singh D J 1994 *Planewaves, Pseudopotentials and the LAPW Method* (London: Kluwer) p 17
- [24] Hamann D R, Schluter M and Chiang C 1979 *Phys. Rev. Lett.* **43** 1494
- [25] Ceperley D M and Alder B J 1980 *Phys. Rev. Lett.* **45** 566
- [26] Segall M, Lindan P, Probert M, Pickard C, Hasnip P, Clark S and Payne M 2002 *J. Phys.: Condens. Matter* **14** 2717
- [27] Fujihisa H 1996 *High Pressure Res.* **14** 335
- [28] Wyckoff R W G 1963 *Crystal Structures* 2nd edn (New York: Interscience) p 52
- [29] Fujii Y, Hase K, Ohishi Y, Fujihisa H, Hamaya N, Takemura K, Shimomura O, Kikegawa T, Ameniya Y and Matsushita T 1989 *Phys. Rev. Lett.* **63** 536
- [30] Fujihisa H, Fujii Y, Takemura K and Shimomura O 1995 *J. Phys. Chem. Solids* **56** 1439
- [31] San-Miguel A, Libotte H, Gauthier M, Aquilanti G, Pascarelli S and Gaspard J P 2007 *Phys. Rev. Lett.* **99** 015501
- [32] Wallace D C 1972 *Thermodynamics of Crystals* (New York: Wiley) p 315
- [33] Riggelman B M and Drickamer H G 1963 *J. Chem. Phys.* **38** 2721